

# CHEMISTRY

---

## AN ASIAN JOURNAL

www.chemasianj.org

### Accepted Article

**Title:** Spontaneous Nanobelt Formation by Self-Assembly of  $\beta$ -benzyl GABA

**Authors:** Hee-Seung Lee, Aram Jeon, Jintaek Gong, Jun Kyun Oh, Sunbum Kwon, Wonchul Lee, Sang Ouk Kim, and Sung June Cho

This manuscript has been accepted after peer review and appears as an Accepted Article online prior to editing, proofing, and formal publication of the final Version of Record (VoR). This work is currently citable by using the Digital Object Identifier (DOI) given below. The VoR will be published online in Early View as soon as possible and may be different to this Accepted Article as a result of editing. Readers should obtain the VoR from the journal website shown below when it is published to ensure accuracy of information. The authors are responsible for the content of this Accepted Article.

**To be cited as:** *Chem. Asian J.* 10.1002/asia.201900363

**Link to VoR:** <http://dx.doi.org/10.1002/asia.201900363>

A Journal of



A sister journal of *Angewandte Chemie*  
and *Chemistry – A European Journal*

---

WILEY-VCH

## COMMUNICATION

# Spontaneous Nanobelt Formation by Self-Assembly of $\beta$ -benzyl GABA

Aram Jeon,<sup>†‡[a]</sup> Jintaek Gong,<sup>†[a]</sup> Jun Kyun Oh,<sup>[b]</sup> Sunbum Kwon,<sup>[c]</sup> Wonchul Lee,<sup>[a]</sup> Sang Ouk Kim,<sup>[d]</sup> Sung June Cho,<sup>[e]</sup> and Hee-Seung Lee<sup>\*[a]</sup>

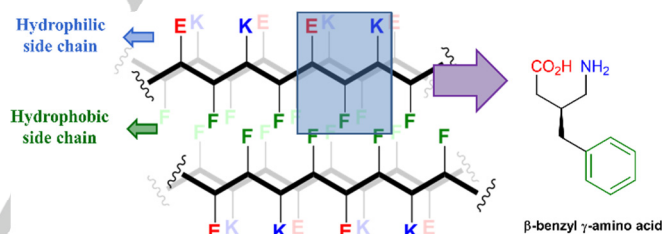
**Abstract:** We present the formation of a nanobelt by self-assembly of  $\beta$ -benzyl GABA ( $\gamma$ -aminobutyric acid). This simple  $\gamma$ -amino acid building block self-assembled to form a well-defined nanobelt in chloroform solvent. The nanobelt showed distinct optical properties due to  $\pi$ - $\pi$  interactions. This new-generation self-assembled single amino acid may serve as a template for functional nanomaterials.

The majority of scientific research on the self-assembly of amyloid  $\beta$  ( $A\beta$ ) has been conducted from a pathological point of view, because the self-assembly of  $A\beta$  is closely related to Alzheimer's disease.<sup>[1]</sup> In particular, numerous studies have been devoted to inhibiting the formation of amyloid fibrils *in vivo* and *in vitro*, in order to overcome this chronic neurodegenerative disease.<sup>[2]</sup> Interestingly, this self-assembly phenomenon has also evoked interest in an entirely different field of research, as chemists have identified useful structural properties of amyloid fibrils. The formation of fibrils under conditions found inside living organisms has inspired chemists to produce well-defined nano-/micro-sized functional materials with amyloid-like peptides.<sup>[3]</sup>

The building block commonly used in these studies is an amphipathic peptide with alternating hydrophobic and hydrophilic residues, usually represented as  $(XZXZ)_n$ .<sup>[4]</sup> The well-known  $\beta$ -strand forming  $(FKFE)_n$  peptides are chains in which hydrophobic (phenyl) and hydrophilic (ammonium and carboxylate) functional groups are positioned in an alternating fashion. Thus, various functional materials using the  $(FKFE)_n$  peptide have been

reported as they readily self-assemble into well-defined superstructures. This is realized in the bilayer structure, which is the representative structure formed spontaneously via self-assembly of amphipathic peptides<sup>[3d, 4b, 4d, 5]</sup>

However, the inherent structural complexities of peptides, such as backbone flexibility and ill-defined secondary structures, remain crucial hurdles in their effective application as building block molecules. This has led to increasing demand for the development of simpler building blocks with low molecular weight that are capable of producing well-ordered supramolecular structures with manipulable assembly mechanisms. In particular, single amino acids are suitable for meeting this demand because they allow simple and cost-effective experimental procedures for self-assembly experiments.<sup>[6]</sup> This attempting to implement a complex self-assembled system using a simpler building block is a common issue in bottom-up approach, and not limited to peptide self-assembly studies,<sup>[7]</sup> indeed. In this vein, some sets of molecules have been reported previously to form a supramolecular structure of a single amino acid; however they require an additional protecting group or a specific condition, such as evaporation of the solution on a surface.<sup>[8]</sup>



**Scheme 1.** Molecular design of the building block for self-assembly, inspired by the typical bilayer structure of  $(FKFE)_n$  peptide. Here, F, K and E represent the side chains of phenylalanine, lysine and glutamic acid, respectively. The backbone structure of  $(FKFE)_n$  peptide is shown as the bold solid-line.  $\beta$ -benzyl GABA ( $\beta$ -benzyl  $\gamma$ -aminobutyric acid,  $\gamma$ -Phe) has all key functional groups similar to  $(FKFE)_n$  peptide (Ph,  $NH_2$ , and  $COOH$ ).

Herein, we introduce a simple  $\gamma$ -amino acid building block,  $\beta$ -benzyl GABA ( $\beta$ -benzyl  $\gamma$ -aminobutyric acid,  $\gamma$ -Phe), that is designed to mimic the fragment of the bilayer structure of amphipathic  $(FKFE)_n$  peptides (Scheme 1). As shown in the scheme, it is proposed that functional groups present in glutamic acid and lysine could be extracted as carboxylic acid and amino groups respectively, as present in the backbone of  $\gamma$ -amino acid. In addition, by maintaining the benzyl group, all functional groups of the tri-peptide FKE can be installed in a single amino acid. This would be the smallest building block that has all the advantages of the amphipathic. Subsequently, it was found that this building block forms well-defined nanobelts with photoluminescence properties, through a spontaneous self-assembly process.

This  $\gamma$ -amino acid, (S)- $\gamma$ -Phe, was synthesized in an enantiopure form by following the procedure given in an earlier study (see ESI for the detailed procedure).<sup>[9]</sup> When a solution of (S)- $\gamma$ -Phe (10  $\mu$ L, 8 g  $L^{-1}$  in ethanol) was added to chloroform (1

- [a] Dr. A. Jeon<sup>†</sup>, Dr. J. Gong, Dr. W. Lee, Prof. H.-S. Lee  
Department of Chemistry  
Center for Multiscale Chiral Architectures (CMCA)  
KAIST  
291 Daehak-ro, Yuseong-gu, Daejeon 34141 (Republic of Korea)  
<sup>†</sup>Current address ; Organic Materials Lab., Materials Center, SAIT,  
SEC, 130 Samsung-ro, Yeongtong-gu, Suwon-si, Gyeonggi-do  
16678 (Republic of Korea)  
E-mail: hee-seung\_lee@kaist.ac.kr
- [b] Prof. J. K. Oh  
Department of Polymer Science and Engineering  
Dankook University  
152 Jukjeon-ro, Suji-gu, Yongin-si, Gyeonggi-do 16890 (Republic of Korea)
- [c] Prof. S. Kwon  
Department of Chemistry  
Chung-Ang University  
84 Heukseok-ro, Dongjak-gu, Seoul 06974 (Republic of Korea)
- [d] Prof. S. O. Kim  
Department of Materials Science and Engineering  
KAIST  
291 Daehak-ro, Yuseong-gu, Daejeon 34141 (Republic of Korea)
- [e] Prof. S. J. Cho  
Department of Applied Chemical Engineering  
Chonnam National University  
77 Yongbong-ro, Buk-gu, Gwangju 61186 (Republic of Korea)

Supporting information for this article is given via a link at the end of the document.

## COMMUNICATION

mL), it self-assembled spontaneously to form well-defined nanobelts within a few minutes of sonication (Figure 1), whereas natural  $\alpha$ -Phe did not undergo self-assembly under the same conditions. Scanning electron microscopy (SEM) images of the filtered material shows fairly homogeneous nanobelt morphology with the length ranging from tens to hundreds of micrometers (Figure 1a–b). The width of the nanobelts is in the range of 0.1–1  $\mu\text{m}$  and the thickness of the nanobelts is about half the width, as shown in the cross-sectional SEM image in Figure 1c. When self-assembly takes place in presence of phosphotungstic acid (used for negative staining in TEM analysis), identical nanobelts are formed. Several parallel dark lines are clearly seen along the axis of the nanobelt in the TEM image (Figure 1d). The occurrence of these dark lines, with a period of 5–10 nm, is probably due to the adhesion of the staining reagent along the hydrophilic region of the nanobelts.

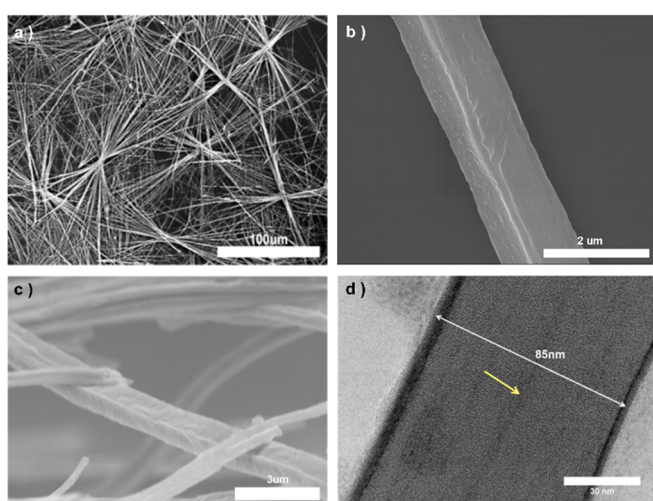


**Figure 1.** a, b) SEM images and c) a cross-sectional SEM image, of the self-assembled structures of  $\gamma$ -Phe. d) High-resolution TEM image of co-assembled structures of  $\gamma$ -Phe with staining reagent (phosphotungstic acid); parallel dark lines are clearly seen in the image (yellow arrow).

To investigate the molecular packing structure of  $\gamma$ -Phe monomers in the self-assembled nanobelts, powder X-ray diffraction (PXRD) analysis of the nanobelts and the raw powder was carried out. Both samples showed considerably strong and distinct peaks, indicating high crystallinity. Unfortunately, the diffraction pattern of the nanobelts could not be indexed with a single-phase unit cell. However, it should be noted that the diffraction pattern of the nanobelts has all diffraction peaks corresponding to the raw powder. This indicates that the molecular packing structure of the nanobelts is either a supercell structure of the raw powder, or that the raw powder is present as an impurity phase in the sample. In other words, the nanobelts are expected to have a packing structure identical to that of the raw powder, with small differences in the conformation such as in the orientation of aromatic rings or the existence of disorders. Thus, we approximated the molecular packing structure of the nanobelts from the raw  $\gamma$ -Phe monomer powder (Figure S1). For the raw powder, a monoclinic unit cell with  $a = 7.966 \text{ \AA}$ ,  $b = 6.400 \text{ \AA}$ ,  $c = 10.4242 \text{ \AA}$ , and  $\beta \approx 90^\circ$  was found to be a probable candidate with a moderately high figure of merit value (F.O.M = 55.7<sup>[10]</sup>). This structure was further refined and its symmetry lowered to have a triclinic unit cell containing a pseudo-2<sub>1</sub> screw

axis along the  $b$ -axis (see ESI for detailed information) during the final Rietveld refinement step. The March-Dollase preferred orientation model<sup>[11]</sup> was adopted for the [100] and [010] axes to approximate the morphological characteristic of the raw powder, which consisted of both plate-like and needle-like structures (Figure S1). The refinement converged to give  $R_p = 8.16 \%$ ,  $R_{wp} = 10.69 \%$ , and  $R_{exp} = 4.89 \%$ , and the obtained March-Dollase preferred orientation coefficients ( $P_{MD}$ )<sup>[11]</sup> were found to be 0.639 and 1.517 along the [100] and [010] directions, respectively. The diffractometer was used in the Bragg-Brentano geometry, and the characteristic morphology of the raw powder was presumed to have produced a strong texture on the sample. The refined structure (Figure 2c) revealed a unique network in the  $ab$  plane, consisting of two orthogonal hydrogen bonds along the  $a$  and  $b$  axes. No typical  $\pi$ - $\pi$  interactions were found inside this structure.

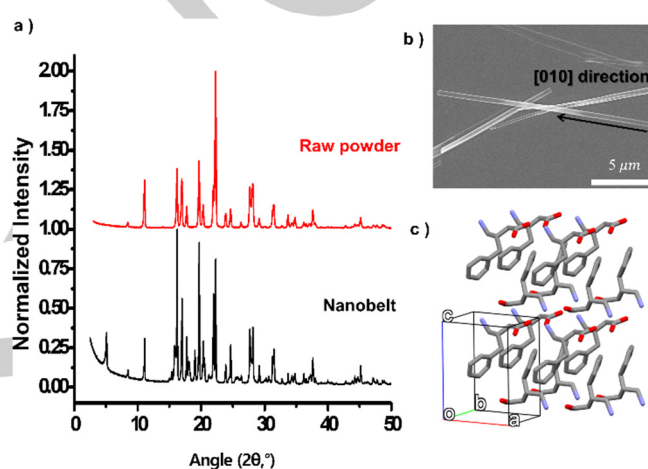


**Figure 2.** a) PXRD patterns of  $\gamma$ -Phe raw powder and nanobelt, b) SEM image of the self-assembled structures of  $\gamma$ -Phe. They have a preferred orientation along the [010] direction. c) The refined structure of  $\gamma$ -Phe monomer in the raw powder form.

Based on the morphological similarity with the needle-like structure of the raw powder, and by the comparison of PXRD patterns and PMD values, it was predicted that the longitudinal direction of the nanobelts would be parallel to the [010] direction (Figure 2, S1). Nonetheless, the cause of the formation of a well-defined structure for the nanobelts during the self-assembly process, in contrast with the raw powder, remained obscure. We hypothesized that there are additional intermolecular and  $\pi$ - $\pi$  interactions in the nanobelt structure that explain this difference in behavior. These interactions can be realized in the nanobelt by the possible aggregation of two phenyl rings in the unit cell in a head-to-tail arrangement to form a  $J$ -dimer.

To confirm the PXRD results, absorption and photoluminescence (PL) measurements were carried out. The absorption spectrum of the nanobelt structure, in which phenyl rings are expected to be well-aligned, is significantly different from that of the raw powder (Figure 3a). While a typical absorption peak (located at 257 nm) due to the aromatic ring of  $\gamma$ -Phe residue is observed for the raw powder (red line), a broad absorption feature centered below 250 nm with tails extending beyond our measurement range is observed for the nanobelts (black line). This demonstrates a clear tendency towards aromatic stacking along the longitudinal axis of an ordered 2D-structure in the nanobelts.

For internal use, please do not delete. Submitted\_Manuscript

## COMMUNICATION

In addition, the nanobelts display different PL properties from that of the raw powder (Figure 3b). Upon excitation at 260 nm (the excitation wavelength of phenyl group), the characteristic peak corresponding to the phenyl ring is found at 280 nm, whereas an additional broad peak appears in the range of 350–450 nm only for the nanobelts. To further investigate the nature of PL in the nanobelts, we obtained the photoluminescence excitation (PLE) spectra at two emission wavelengths of 280 nm and 395 nm (blue and black lines in Figure 3c, respectively). The first excitation spectrum (blue line) exhibits a sharp peak centered at about 260 nm, which corresponds to the aforementioned inherent property of aromatic rings. On the other hand, the second spectrum (black line) reveals that the center of the emission peak for a 395 nm excitation is located at a wavelength of 330 nm. Thus, when the excitation wavelength is 260 nm, the PL spectrum of the nanobelts has a relatively lower intensity for the 395 nm peak compared to the 280 nm peak, as seen in Figure 3b. Figure 3d shows a comparison of PL intensity with the excitation wavelengths 330 nm (black line) and 260 nm (blue line). The peak intensity at 395 nm is three times stronger than at 280 nm. These features of the PL spectra can be observed in polymer compounds containing aromatic groups due to the transition of the  $\pi^*$  excited state to the  $\pi$  state. The broad excitation and emission bands may indicate the existence of several “conjugation lengths” (the degree of  $\pi$ -stacking of  $\gamma$ -Phe) with various HOMO–LUMO energy band gaps in the nanobelts.

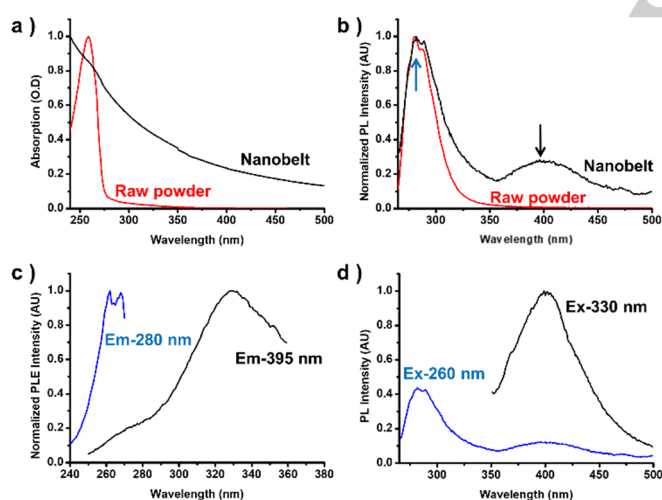


**Figure 3.** a) Absorption spectra of  $\gamma$ -Phe nanobelt (black line) and  $\gamma$ -Phe raw powder (red line). b) PL spectrum (excitation wavelength: 260 nm) of  $\gamma$ -Phe nanobelt (black line) and  $\gamma$ -Phe raw powder (red line). There are two distinct peaks in for the nanobelt: a sharp peak located at 280 nm (blue arrow) and a broad peak located at 395 nm (black arrow). c) PLE spectrum of  $\gamma$ -Phe nanobelt obtained while detecting the emission at two wavelengths: 395 nm (black line) and 280 nm (blue line). d) PL spectrum of  $\gamma$ -Phe nanobelt at two excitation wavelengths: 330 nm (black line) and 260 nm (blue line).

All these experimental results lead us to the conclusion that the conformational preorganization of  $\gamma$ -Phe through intramolecular hydrogen bonding plays an important role in accelerating and guiding the self-association in the solution phase. This is achieved by considerably reducing the entropic cost that must be overcome to form the preferred linear ordering. The  $\pi$ – $\pi$  interactions also play a crucial role and are well-balanced with hydrogen bonding in association with the building blocks.

Additional control experiments proved that the existence of the phenyl group for  $\pi$ – $\pi$  interaction was necessary to form the well-defined nanostructures, such as nanobelt shape in this case. This is clearly supported by the self-assembly studies using other  $\gamma$ -amino acids ( $\beta$ -isobutyl-GABA (pregabalin) and gabapentin) with aliphatic side chains. None of the cases provided well-defined structures, as shown in Figure S8.

In conclusion, we present an interesting example for producing well-defined nanomaterials with cost-efficient building blocks. The  $\beta$ -benzyl GABA used in this study revealed a characteristic of efficient self-assembly into a nanobelt structure containing fibrillar bilayers similar to that of the amphipathic (FKFE)<sub>n</sub> sequence. Additionally, the single amino acid self-assembles spontaneously into well-defined nanobelts with PL properties due to the  $\pi$ -conjugated system. We have thus presented an example illustrating how to design a bio-inspired, molecular building block for effective and spontaneous association by introducing the requisite functional groups in a proper geometry and conformation. It is expected that the present results will lend new insight into the design principle of molecular building blocks for functional complex nanostructures by self-assembly from a cost-efficiency point of view. In addition, this strategy of using amyloid-inspired peptides for nano-engineering can be applied to multiple fields such as biomedicine, tissue engineering, wound healing, and drug delivery.

## Acknowledgements

† A. Jeon and J. Gong contributed equally to this work. We thank Mr. Joo Min Kim and Ms. Danim Lim (KAIST) for assistance in preparing this manuscript. This research was supported by National Research Foundation (NRF) of Korea grant funded by the Ministry of Science and ICT (2016R1A2A1A05005509, 2018R1A5A1025208).

**Keywords:** Self-assembly • Nanostructure • Amino acid • Photoluminescence

- [1] a) O. S. Makin, L. C. Serpell, *FEBS J.* **2005**, *272*, 5950–5961; b) F. Chiti, C. M. Dobson, *Annu. Rev. Biochem.* **2006**, *75*, 333–366; c) M. Fändrich, *Cell. Mol. Life Sci.* **2007**, *64*, 2066–2078; d) L.-M. Yan, A. Velkova, M. Taterek-Nossol, E. Andreetto, A. Kapurniotu, *Angew. Chem. Int. Ed.* **2007**, *46*, 1246–1252; e) J. Habchi, S. Chia, C. Galvagnion, T. C. T. Michaels, M. M. J. Bellaiche, F. S. Ruggeri, M. Sanguanini, I. Idini, J. R. Kumita, E. Sparr, S. Linse, C. M. Dobson, T. P. J. Knowles, M. Vendruscolo, *Nat. Chem.* **2018**, *10*, 673–683.
- [2] a) N. Gao, H. Sun, K. Dong, J. Ren, X. Qu, *Chem. Eur. J.* **2014**, *21*, 829–835; b) S. I. A. Cohen, P. Arosio, J. Presto, F. R. Kurudenkandy, H. Biverstäl, L. Dolfe, C. Dunning, X. Yang, B. Frohm, M. Vendruscolo, J. Johansson, C. M. Dobson, A. Fisahn, T. P. J. Knowles, S. Linse, *Nat. Struct. Mol. Biol.* **2015**, *22*, 207–213; c) A. J. Doig, P. Derreumaux, *Curr. Opin. Struct. Biol.* **2015**, *30*, 50–56; d) N. Xiong, X.-Y. Dong, J. Zheng, F.-F. Liu, Y. Sun, *ACS Appl. Mater. Interfaces* **2015**, *7*, 5650–5662; e) W.-J. Du, J.-J. Guo, M.-T. Gao, S.-Q. Hu, X.-Y. Dong, Y.-F. Han, F.-F. Liu, S. Jiang, Y. Sun, *Sci. Rep.* **2015**, *5*, 7992; f) A. Francioso, P. Punzi, A. Boffi, C. Lori, S. Martire, C. Giordano, M. D’Erme, L. Mosca, *Bioorg. Med. Chem.* **2015**, *23*, 1671–1683; g) T. Su, T. Zhang, S. Xie, J. Yan, Y. Wu, X. Li, L. Huang, H.-B. Luo, *Sci. Rep.* **2016**, *6*, 21826; h) X.-L. Bu, P. N. Rao, Y.-J. Wang, *Mol. Neurobiol.* **2016**, *53*, 3565–3575.
- [3] a) G. Wei, Z. Su, N. P. Reynolds, P. Arosio, I. W. Hamley, E. Gazit, R. Mezzenga, *Chem. Soc. Rev.* **2017**, *46*, 4661–4708; b) S. Das, R. S.

For internal use, please do not delete. Submitted\_Manuscript

## COMMUNICATION

- Jacob, K. Patel, N. Singh, S. K. Maji, *Biomacromolecules* **2018**, *19*, 1826–1839; c) I. Cherny, E. Gazit, *Angew. Chem. Int. Ed.* **2008**, *47*, 4062–4069; d) T. P. J. Knowles, R. Mezzenga, *Adv. Mater.* **2016**, *28*, 6546–6561.
- [4] a) C. J. Bowerman, B. L. Nilsson, *Biopolymers* **2012**, *98*, 169–184; b) R. J. Betush, J. M. Urban, B. L. Nilsson, *Pept. Sci.* **2018**, *110*, e23099; c) J. Mangelschots, M. Bibian, J. Gardiner, L. Waddington, Y. Van Wanseele, A. Van Eeckhaut, M. M. D. Acevedo, B. Van Mele, A. Madder, R. Hoogenboom, S. Ballet, *Biomacromolecules* **2016**, *17*, 437–445; d) D. Li, E. M. Jones, M. R. Sawaya, H. Furukawa, F. Luo, M. Ivanova, S. A. Sievers, W. Wang, O. M. Yaghi, C. Liu, D. S. Eisenberg, *J. Am. Chem. Soc.* **2014**, *136*, 18044–18051.
- [5] a) R. J. Swanekamp, J. T. M. DiMaio, C. J. Bowerman, B. L. Nilsson, *J. Am. Chem. Soc.* **2012**, *134*, 5556–5559; b) K. Matsuura, *Chem. Commun.* **2018**, *54*, 8944–8959.
- [6] a) P. W. J. M. Frederix, G. G. Scott, Y. M. Abul-Haija, D. Kalafatovic, C. G. Pappas, N. Javid, N. T. Hunt, R. V. Ulijn, T. Tuttle, *Nat. Chem.* **2014**, *7*, 30; b) K. Tao, A. Levin, L. Adler-Abramovich, E. Gazit, *Chem. Soc. Rev.* **2016**, *45*, 3935–3953; c) C. Guo, Z. A. Arnon, R. Qi, Q. Zhang, L. Adler-Abramovich, E. Gazit, G. Wei, *ACS Nano* **2016**, *10*, 8316–8324.
- [7] a) M. Yamanaka, *J. Incl. Phenom. Macrocycl. Chem.* **2013**, *77*, 33–48; b) A. J. Kleinsmann, N. M. Weckenmann, B. J. Nachtsheim, *Chem. Eur. J.* **2014**, *20*, 9753–9761; c) B. J. Cafferty, I. Gállego, M. C. Chen, K. I. Farley, R. Eritja, N. V. Hud, *J. Am. Chem. Soc.* **2013**, *135*, 2447–2450; d) A. Jesorka, A. R. Holzwarth, A. Eichhöfer, C. M. Reddy, Y. Kinoshita, H. Tamiaki, M. Katterle, J.-V. Naubron, T. S. Balaban, *Photochem. Photobiol. Sci.* **2012**, *11*, 1069–1080; e) G. Ragazzon, M. Baroncini, S. Silvi, M. Venturi, A. Credi, *Beilstein J. Nanotechnol.* **2015**, *6*, 2096–2104.
- [8] a) P. Koley, A. Pramanik, *Adv. Funct. Mater.* **2011**, *21*, 4126–4136; b) P. Koley, A. Pramanik, *J. Mater. Sci.* **2014**, *49*, 2000–2012; c) C. Ménard-Moyon, V. Venkatesh, K. V. Krishna, F. Bonachera, S. Verma, A. Bianco, *Chem. Eur. J.* **2015**, *21*, 11681–11686; d) P. Chakraborty, E. Gazit, *ChemNanoMat* **2018**, *4*, 730–740.
- [9] T. Ok, A. Jeon, J. Lee, J. H. Lim, C. S. Hong, H.-S. Lee, *J. Org. Chem.* **2007**, *72*, 7390–7393.
- [10] P. M. de Wolff, *J. Appl. Crystallogr.* **1972**, *5*, 243.
- [11] W. A. Dollase, *J. Appl. Crystallogr.* **1986**, *19*, 267–272.

